

# DISTANCE AWARE TRANSMIT ANTENNA SELECTION FOR MASSIVE MIMO SYSTEMS

Shenko Chura<sup>1</sup>, Yalemzewd Negash<sup>1</sup> and Yihenew Wondie<sup>1</sup>

School of Electrical and Computer Engineering, Addis Ababa Institute of Technology, Addis Ababa University, Addis Ababa, Ethiopia

Corresponding Author's Email: [duskaanoo@gmail.com](mailto:duskaanoo@gmail.com)

## ABSTRACT

*Multiple-Input Multiple-Output (MIMO) antenna selection is a signal processing technique by which the Radio Frequency (R.F.) chain components are switched to their corresponding subset of antennas. Antenna selection resolves the complexity and power consumption of R.F. transceivers. This paper proposes an optimal antenna selection technique for multiple radio component type massive MIMO, which combines two selection techniques by exploiting the minimum signal-to-noise ratio (SNR) at the cell edge and dynamic channel condition due to mobility. After an adaptive selection has been made, the same number of R.F. components are active, and the rest are set to sleeping mode to apply fractional transmit power re-allocation at sub 6GHz and mm Wave frequencies. Accordingly, the branch with better signal quality among the array is chosen and added in iteration till the selected value is attained; however, re-selection still boosts E.E. at the cost of the total rate. The results show that the algorithm over performs the random selection, achieving better energy efficiency than full array utilization and random selection. Moreover, capacity reduction due to selection is compensated by applying nonlinear precoding at the cost of complexity.*

**Keywords:** Antenna Selection, Energy Efficiency, Massive MIMO, mm Wave, Precoding

## INTRODUCTION

Massive MIMO (mMIMO) is a large-scale MIMO device gaining popularity in wireless communications that scales up traditional MIMO by orders of magnitude, according to [1]. It takes into account multi-user MIMO, in which a base station with hundreds of thousands of antennas simultaneously supports many single-antenna terminals, as well as frequency resources. Connection reliability, spectrum quality, and radiated energy efficiency all improve when a device has many antenna elements. Each antenna element is linked to a single R.F. chain at the base station, which comprises mixers, analog-to-digital converters (ADC), and amplifiers [2]. Furthermore, the increase in the number of antennas and associated R.F. chains at the base station will result in physical restrictions, complexity, and expense [3]. According to [4], R.F. chains are responsible for approximately 50-80% of a base station's total transceiver power consumption.

As the number of quantization bits and B.S. antenna elements grow, the hardware complexity and power consumption of DACs grows exponentially. As a result, according to [5], adopting a low-resolution DAC is a potential choice. In addition,

conversion from analog to digital and digital to analog (ADC/DAC), phase shifters, and power amplifiers all affect the power amplifier's energy usage. Although the digital beam forming system provides a high data rate, the transceiver system uses the same number of antennas as the chains, resulting in excessive energy usage. On the other hand, a hybrid beamforming system utilizes fewer R.F. components and can provide equivalent spectral efficiency to a digital beamforming system while being more energy-efficient, according to [6].

Although hybrid beam forming is used to employ a small number of R.F. chains as the solution, one of the unanswered concerns is how to reduce some numbers among the whole array. Antenna selection has been employed as one of the power-saving approaches for a system with a vast array of R.F. components. The majority of recent studies in the literature have focused on performance analysis for large MIMO uplinks with low-resolution analog-to-digital converters. In this regard, [7] studied the impact of signal detection strategies on the energy efficiency of uplink MIMO systems with low-resolution analog-to-digital converters. In m MIMO systems, there have been few previous investigations on antenna selection. During the last few decades, various antenna selection strategies and algorithms have been investigated for classic MIMO.

The studies in [8] supported capacity-oriented selection criteria such as the greedy method and convex optimization. In [9], the authors introduced an antenna selection approach (AS) with a low degree of complexity that selects antennas with the least amount of constructive user interference. The suggested AS approach outperforms systems that use a more sophisticated channel inversion method when the transmitter uses precoders in

conjunction with a matched filter. The goal of the work in [10] was to eliminate the destructive fraction of the interference caused by the link between the sub streams of a modulated Phase Shift Keying (PSK) system. Singular value decomposition was used to offer a new Euclidean distance-dependent technique for antenna selection in spatial modulation systems that have a lower computing complexity than an exhaustive search [11]. Furthermore, the Symbol Error Rate (SER) approaches a complete search as the number of received antennas increases. As a result, the authors of [12] noted that, in comparison to previous and current research trends, there is still a lot of interest in mm Wave based massive MIMO antenna selection with less complexity, higher energy efficiency, and optimal data rates in recent years. This paper studies a system with transmit antenna selection for massive MIMO-enabled BS.

The technique is broken down into two sections: First, at the cell edge, a whole array device's energy efficiency (E.E.) is assessed using a fixed power allocation technique that assumes the channel is deterministic. In this scenario, the initial access condition is used to find the optimal number of B.S. antennas where the E.E. reaches its maximum. Second, as users go from the cell edge to the outskirts or center places, the minimum Signal to Noise Ratio (SNR) found at the cell edge is employed as a threshold value to further search for the ideal number.

To find is utilized as the total number of B.S. antennas. Then, the Free Space (F.S.) Path Loss (P.L.) model is employed for each mobile terminal, with adaptive power allocation based on minimum SNR at the cell edge. After determining, the subset of antennas with the best channel conditions is chosen, and E.E. is evaluated using spatial selectivity at mm Wave frequency ranges.

The following are the primary contributions of this paper:

Although our selection algorithm also shows that when partially applying the same exhaustive search technique, the complexity, and energy efficiency decrease and increase respectively due to double selection before exhaustive search.

- We derive a mathematical formulation for energy-efficient antenna selection.
- We evaluate the performance of mmWave based mMIMO antenna selection with and without nonlinear precoder from the perspective of energy efficiency.
- In comparison to prior methods, we analyze the computational complexity of the proposed transceiver system.

The rest of the work is structured as follows: A system model for mMIMO beam forming and array geometry is defined in section II. After the propagation model is explained in section III, antenna selection and power consumption models are followed in sections IV and V, where results and analysis are done. Finally, conclusions are drawn in section VI.

### SYSTEM DESCRIPTION

The system description is divided into two parts. First the signal model of a downlink massive MIMO system with transmit antenna selection is outlined. Then the addressed antenna selection technique is defined and formulated for a sub-optimal solution.

### System Model

Here, the channel model with only free space non-fading (i.e., pure) LoS propagation between the B.S. and the devices is presented; that the B.S. is fitted with a ULA with a  $\lambda/2$  spaced  $M$  antenna portion where  $\lambda$  is the signal wavelength where the presence of the mutual coupling effect between antenna elements is not taken in to account. There are randomly distributed  $K$  single-antenna devices inside the cell that simultaneously transmit data to the B.S. using the same time-frequency resources. Furthermore, it is also assumed that all of the  $K$  devices served by the B.S. are positioned at various angles on the far-field of the antenna array and undergo fading of large and small scales. Downlink  $M^o$  RF chains associated with  $K(K \leq M^o \leq M)$  are considered for a single-cell massive MIMO structure.

### Mobile Location Positioning

Mobile Location Positioning in today's cellular networks, identifying a mobile position is a critical problem. The angle of Arrival (AoA), Time of Arrival (ToA), and GPS are among the techniques used. In general, there are three methods for determining the location of a mobile terminal: satellite positioning, cellular network-based positioning, and indoor positioning. The trilateration method is used to calculate a mobile's location using a relative position of a base station (B.S.). Unlike the triangulation process, which requires the angle of each user for position tracking, only the distance between the B.S. and each user is required in this case [24].

### Close-In (CI) path loss model

The CI model is based on Friis and Bullington's fundamental radio propagation concepts, wherein the value is 2 for free space and 4 for the asymptotic two-ray ground bouncing model. It provides insight

into path loss as a function of the environment since base station towers are tall and inter-site distances for specific frequency bands are several kilometers. Previous UHF/microwave models employed a close-in standard distance of 1 km or 100m [12]. The CI 1m reference distance, as proposed in [13], is a suitable recommended norm that relates the real transmit power or PL to a reasonable distance of 1m. Standardization to a 1m reference distance simplifies dimension and model comparisons, provides a consistent description for Path Loss Exponent (PLE) and allows for quick and straightforward route loss estimates without the need for a calculator [14]. Using power control mechanisms, user terminals nearer to the BS are allocated lower power than those on the outskirts to control interference and fairness. CI path loss model is a generic frequency model that explains large-scale path loss at all applicable frequencies in a specific context. The dynamic range of signals perceived by users in a commercial system becomes significantly lower than the equation for the CI model, which is formulated as [ 12]

$$PL_{CI}(\cdot)_{dB} = PL_{FS}(f, 1m) + 10\log_{10}(d) + \chi_a^{CI} \quad (1)$$

Where  $n = \sum(DA) / \sum(D^2)$ , denotes a single model criterion, the PLE, with 10n defining path loss in dB in terms large distance starting from 1m and (.) represents frequency and distance parameters. The free space path loss,  $PL_{FS}(f, 1)_{dB}$  at 1m distance from a station and carrier frequency f.  $A = PL_{CI}(\cdot)_{dB} - PL_{FS}(f, 1m)$ ,  $10\log_{10}d$  denotes a single model criterion, the PLE, with 10n defining path loss in dB in terms large distance starting from 1m and (.) represents frequency and distance parameters. The free space path loss,  $PL_{FS}(f, 1)_{dB}$  at 1m distance from a station and carrier frequency f is given as

$$PL_{FS}(f, 1m)[dB] = 20\log_{10}(4\pi/\lambda) \quad (2)$$

where  $\lambda$  is wavelength of the signal. It's worth noting that the CI model includes an intrinsic frequency interdependence of path loss in the 1m  $PL_{FS}$  value, and it only has one parameter compared to the ABG  $\alpha$ ,  $\beta$ , and  $\gamma$  model where  $\alpha$  and  $\gamma$  are coefficients showing the dependence

of path loss on distance and frequency, respectively and  $\beta$  is an optimized offset value for path loss in dB.  $\sigma^{CI} = \sqrt{\sum \chi_{\sigma}^{CI^2} / T}$  where T is the number of data points.

Table 1 shows the frequency ranges to be used in CI pathloss model in urban micro for street canyon (UMi-SC) and open space (UMi-OS) at line of sight (LOS) and non-line of sight (NLOS) conditions respectively [14]. As shown in the table, the CI model provides path loss exponent (PLE) of 2.0 and 1.9 in LOS, which approaches well with a free space PLE of 2.

Table 1:Close-in path loss model parameters

Scenario	Freq. (GHz)	Distance (m)	PL E/ $\alpha$	$\alpha^{CI}$
UMi-SC LOS	2-73.5	5-121	2.0	2.9
UMi-SC NLOS	2-73.5	19-272	3.1	8.0
UMi-OS LOS	2-60	5-88	1.9	4.7
UMi-OS NLOS	2-73.5	8-235	2.8	8.3
UMa LOS	2-73.5	58- 930	2.0	4.6
UMa NLOS	2-73.5	45-1429	2.7	10.0

### Trilateration Based Antenna Selection

In the selection process, the number of antennas to be selected is decided by adjusting the sufficient amount of transmit power to be radiated through only the

## Distance Aware Transmit Antenna Selection for Massive MIMO Systems

selected number of antennas. Trilateration is used to find a user's location so that the main beam can focus only on the desired location to minimize leakage. Due to user mobility, the transmit power adaptively changes as user position varies as a distance function. In this case, considering the minimum SNR at the cell edge as a threshold value, the number of transmit antennas can be reduced adaptively when the user comes closer to the center of the BS instead of using all arrays that may lead to unnecessary power wastage. In contrast, the BS only allocates the power proportional to the reduced distance to the maximum transmit power allocation concerning edge distance. Hence, only a few antennas are activated, as stated in (3). Then, the antennas with better channel gains are selected among the array using factorial permutations  ${}^M C_N$  as

$$M^o = \frac{M \cdot \sum_{i=1}^K p_t / K}{P_T} \quad (3)$$

where  $p_t$  is the transmit power adjusted for each user based on path loss,  $P_T$  is the total transmit power and  $N = M^o$  is the number of RF chain components. The selection process for the whole system is stated in a sub optimal algorithm 1 and 2 below.

**Algorithm 1:** Initial access based optimal number selection algorithm

**Input:**  $D_{max}$ ,  $M$ ,  $K$ ,  $f$ ,  $\gamma$ ,  $p_t$ ,  $B$ ,  $p_{amp}$ ,  $p_{bb}$ ,

$p_{syn}$ ,  $p_{dac}$ ,  $p_{mix}$ ,  $p_{filt}$

**Output:** EE,  $M^*$ ; \*/

**begin**

- 1  $\zeta = 0$ ,  $\hat{p}_t = 30mW$ ,  $D_{max} = 300m$ ;
- 2 **for**  $l = 1 : \text{length}(M)$  **do**
- 3  $H \leftarrow (\text{randn}(K, l) + j(\text{randn}(K, l)))$
- 4  $\zeta(l) = \log_2(\text{real}(\det(I + (\frac{\gamma^{sel}}{l})H H^t)))$
- 5  $p_{tot(l)} \leftarrow p_{amp} + (p_{bb} + p_{syn}) + (l(p_{dac} + p_{mix} +$

$p_{filt}))$ ;

- 6  $EE \leftarrow \frac{\zeta(l)}{p_{tot(l)}}$
- 7 **if**  $l = M_{max}$  **then**
- 8  $M^* \leftarrow l$  ( $\text{find}(EE == \max(EE))$ )

In algorithm one, the parameters in each line are represented as follows:

- The outputs are energy efficiency and optimal number of antennas at cell edge respectively;
- In line 2,  $D_{max}$  is cell edge distance;
- $\zeta(l)$  in line 5 is capacity in each iteration;
- $p_{tot(l)}$  is total power in each iteration;

**Algorithm 2:** Number and element selection after reduced distance

**Input:**  $d_{min}$ ,  $\gamma$ ,  $p_t$

**Output:** EE,  $M^o$

**begin**

- 1 re-trilateration: **for**  $i \in k$  **do**
- 2  $r_k \leftarrow R(k_i)$
- 3 **if**  $r_k \neq d_{min}$  **then**
- 4  $P_{rmin} \leftarrow P_{tmax} / \Gamma(R)$
- 5  $P_r(k) \leftarrow \Gamma_r P_{rmin}$
- 6  $M_1^o = \frac{M \cdot \sum_{i=1}^k P_t / K}{P_T}$
- 7  $M_2^o \leftarrow \frac{\text{round}(\sum(\Gamma(r)) / K) M}{\Gamma(R)}$
- 8 **if**  $M_1^o \neq M_2^o$  **then**
- 9 **goto** re-trilateration
- 10  $M_1^o \leftarrow M_2^o$
- 11 **for**  $\gamma = 1 : M^o$  **do**
- 12  $\Psi = \text{rand}(K; M) + j\text{rand}(K, M)$
- 13  $H = \frac{\Psi}{\sqrt{M^o}}$ ;
- 14 **for**  $M_i^o = 1 : M^o$  **do**
- 15  $H_c = [H ; [M_i^o \quad M - i]]$
- 16  $\Phi = \det(I + \gamma * H_c * H_c^t)$
- 17  $\zeta(m) = \log_2(\text{real}(\Phi))$
- 17  $\zeta_{max} = \max(\zeta(m))$

18  $M_i^0 \leftarrow \text{find}(\zeta = \zeta_{max})$   
 19  $\zeta(\gamma) \leftarrow \zeta_{max}$   
 20  $EE \leftarrow \frac{\zeta(\gamma)}{p_{tot}} ;$

In algorithm one, the parameters in each line are represented as follows:

- The outputs are minimum distance, fixed SNR and total transmit power respectively;
- $r_k$  in line 3 is the random distance of a user;
- $\Gamma(R), \Gamma(r)$  in line 8 is path loss in dB at cell edge and reduced distance;
- $Pr_{min}$  in line 5 is minimum received power at the cell edge;
- $P_r(k)$  in line 6 is received power at a k user;
- EE in line 22 energy efficiency with selected branches and total power;
- $M_1^0$  in line 7 is the number of optimal antennas at reduced distance;

### Energy Efficiency Evaluation

With chosen antennas  $M^o$ , among M, the transceivers corresponding to  $M^o$  are turned on while some M - $M^o$  's shut off. With massive MIMO, the number of BS antennas (M) is assumed to be always much greater than the number of single antenna user terminals ( $M \gg K$ ) and allow  $M^o$  to be within the range from K to M. Where  $M^o$ , K is the number of antennas to be chosen and the total number of user terminals with a single antenna respectively. The downlink-channel model is

$$y_l = \sqrt{\rho K} H_l^{(M^o)} z_l + n_l. \quad (4)$$

Where  $H_l^{M^o}$  is a  $K \times M^o$  channel matrix on carrier  $l$  and the  $M^o$  subscript indicates that antenna selection has been made, i.e.,  $M^o$  columns of  $H_l^{M^o}$  are chosen from the complete channel matrix of  $K \times M$ .

### Dirty Paper Coding Sum Capacity ( $C_{(DPC)}$ )

The downlink sum-capacity at subcarrier is given by [6]:

$$C_{DPC_l} = \max_{P_l} \log_2 \det (I + \rho K (H_l^{(N)})^H P_l H_l^{(N)}) \quad (5)$$

In (5),  $P_l$  is a diagonal power allocation matrix with  $P_{l,i}$   $I = 1, 2, \dots, K$  on its diagonal. And the optimization is also carried out according to the total power restriction of  $\sum_{i=1}^K P_{l,i} = 1$  as in (5). This problem of optimization is convex, and can be solved, for example, by using the water-filling algorithm of sum-power iterative. DPC is highly complex to implement in practice. However, there are suboptimal linear precoding schemes, such as zero-forcing (ZF) precoding that is much less complex and performs fairly well for massive MIMO [15].

### Zero Forcing Sum Capacity ( $C_{\{ZF\}}$ )

The total rate achieved by ZFT is [15]

$$C_{ZF,l} = \max_{Q_l} \sum_{i=1}^K \log_2 (1 + \rho K Q_{l,i}) \quad (6)$$

Where  $Q_{l,i}$  represents SNRs obtained by the various users and the maximization is carried out according to the total power constraint

$$\sum_{i=1}^K Q_{l,i} \left[ \left( H_l^{(N)} (H_l^{(N)})^H \right)^{-1} \right] = 1 \quad (7)$$

In (6) and (7),  $Q_l$  is a diagonal matrix with  $Q_{l,i}$   $i=1, 2, \dots, K$  in its diagonal, and  $[.]_i$  means the matrices  $I$  diagonal. The  $\left( H_l^{(N)} (H_l^{(N)})^H \right)^{-1}$  diagonal elements reflect the power penalty of null-out intervention.

An  $M \times M$  diagonal matrix of  $\varphi$  with binary diagonal elements has been implemented to

pick the  $N$  columns from the complete MIMO matrix  $H_l$ .

$$\varphi_i = \begin{cases} 1 & \text{Selected} \\ 0 & \text{Otherwise} \end{cases} \quad (8)$$

indicating whether the  $i^{th}$  antenna is selected, and satisfying  $\sum_{i=1}^M \varphi_i = N = M^o$ . Using Sylvester's determinant identity,  $\det(I+AB) = \det(I+BA)$ , the DPC sum capacity in (5) can be re-written in terms of  $\varphi$  as

$$C_{DPC,l} = \max_{P_l} \log_2 \det \left( I + \rho K P_l H_l^{(N)} (H_l^{(N)})^H \right) = \max_{P_l} \log_2 \det \left( I + \rho K P_l H_l \varphi (H_l)^H \right) \quad (9)$$

subject to  $\sum_{i=1}^K P_{l,i} = 1$ .

The optimal  $\varphi$  (common to all subcarriers) is found by maximizing the average DPC capacity,

$$\varphi_{opt} = \max_{\varphi} \frac{1}{L} \sum_{l=1}^L \log_2 \det \left( I + \rho K P_l H_l \varphi (H_l)^H \right) \quad (10)$$

With the subsequent range of antenna, the respective sum-rate of ZF

$$C_{ZF,l} = \max_{Q_l} \sum_{i=1}^K \log_2 (1 + \rho K Q_{l,i}) \quad (11)$$

$$\text{Subject to } \sum_{i=1}^K Q_{l,i} \left[ (H_l^{(N)} (H_l^{(N)})^H)^{-1} \right]_{i,i} = 1 \quad (12)$$

Despite  $\varphi_{opt}$  may not be optimal for ZF, the ZF sum-rate indicates the antenna selection performance when using a more practical precoding scheme than DPC. As discussed above, exhaustive search of all possible combinations of  $N$  antennas will certainly give us the optimal  $\varphi$  however, it is extremely complex and infeasible for massive MIMO. From (11,12), it can be seen that zeroing the upper and lower matrix elements requires additional power consumption in ZF however still it is simpler in processing compared to DPC which has no additional power penalty and complex on the other hand.

### Energy Efficiency Evaluation

The total energy efficiency of the system can be evaluated as [15]:

$$C = KE \left[ \log_2 \left( \left[ 1 + \rho \|g_k\|^2 \right] \right) \right] \quad (13)$$

$$EE = KE \left[ \log_2 \left( 1 + \rho \|g_k\|^2 \right) \right] / P_{total} \quad (14)$$

Where  $P_{total} = P_{amp} + P_{CP}$  and  $P_{CP} = P_{bb} + P_{syn} + M^o * (P_{dac} + P_{mix} + P_{filt})$  where  $P_{CP}$  accounts for the circuit power consumption.  $P_{amp}$  is the amount of the power produced by various analog components. In  $P_{CP}$ , baseband signal processing ( $P_{bb}$ ), synchronization ( $P_{syn}$ ) are independent of number of BS antennas while digital to analogue conversion power ( $P_{dac}$ ), mixing ( $P_{mix}$ ) and filtering ( $P_{filt}$ ) power linearly increase with selected BS antennas. Table 2 contains the parameters to be used for simulation purpose in evaluation of EE according to (14).

Table 2: Complexity Analysis

Algorithm 2	Algorithm 1+2
$\left( \hat{n} \binom{M}{M^o} \right)$	$\left( \hat{n} \binom{M}{M^o - 1^*} \right)$

The table states the combinational permutation of the algorithms which we compare with that of [16], [17], [18] and [19] which accounts for  $\hat{n} \binom{M}{M^o}$  where  $\hat{n} = M^2 + 2M_{o \equiv s}^2 + M^o$  and  $1^*$  is the deducted elements due to selection. According to [17] and [18], the computational complexity due to selection process is shown in (16) and (17) respectively.

$$\mathcal{O}_1(\cdot) = 16n^3 + \hat{n}^2(24M^2 + 40M + 24 - 24M^{o^2} - 24M^o), \quad (15)$$

$$\mathcal{O}_2(\cdot) = \hat{e} + 20(M^2 + M - M^{o^2} - M^o), \quad (16)$$

$$\mathcal{O}_3(\cdot) = \mathcal{O}_1(\cdot) + \mathcal{O}_2(\cdot), \quad (17)$$

$$O_4(.) = \hat{n}(M^{o^2}(M3(M + 1)))(18)$$

Where  $\hat{e} = \hat{n}(34M^2 + 44M - 36M^{o^2} - 34M^o)$  and  $(.)$  denotes  $(M, M^o)$ . In [30] low-complexity transmit antenna selection (LCTAS) was studied and found to have complexity level as follows:

$$O_{[30]} = o(M^o S^o \binom{M}{M^o})(19)$$

where  $S^o$  is the number of symbols for a constellation type.

Table 3: Simulation parameters for the overall work

Parameter	Value	Description
$P_{tx}$	5mW	Transmission power
$p_{mix}$	0.033	Mixing consumption
$p_{filt}$	0.02	Filtering consumption
$p_{bb}$	0.03	Base band signal processing power
$p_{syn}$	0.05	Synchronization power
$p_{dac}$	0.015	Digital to analogue conversion power
$p_{amp} = p_{tx}/\eta$	$\eta=0.01$	Amplifier power
$f_s$	1800 Mhz	Sub 6Ghz frequency
$f_m$	37 Ghz	mmWave band

## RESULTS AND DISCUSSIONS

In figure 1, ergodic capacity of different MIMO configurations for iid (independent identically distributed) channel has been shown. From the figure it can be concluded that, the capacity becomes higher for of massive MIMO with different number of antenna configurations than classical MIMO systems however at lower SNR level the difference is much less and can be neglected. However, increase in the number of BS antennas accounts for increase in SNR

which signifies system's capacity enhancement. In this case, NT represents the number of BS antennas, M.

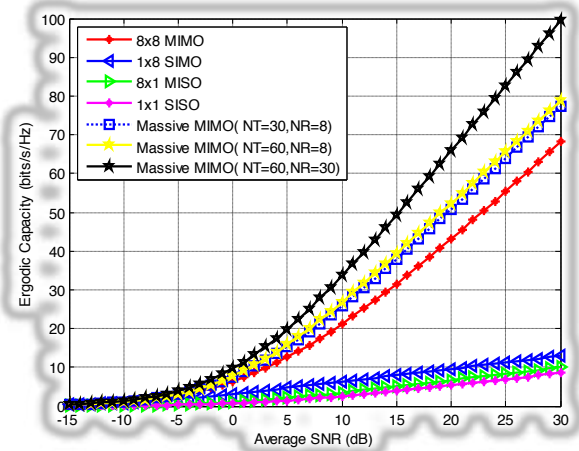


Figure 1: Ergodic Capacity for i.i.d. Rayleigh fast fading channel in different MIMO configurations.

Figure 2 depicts the effect of randomly selected transmit antennas on system energy efficiency. The energy efficiency increases with the number of transmit antennas (M) first, and after an optimal point, it abruptly declines. The increase in BS antennas is directly associated with the rise in the corresponding radio frequency chain components, which accounts for enormous power consumption in a system. From the figure, the optimal number of antennas ( $M^*$ ) also depends on the number of user terminals (K). For K=5, 10,15, and 20,  $M^*=5, 7, 8,$  and 9.

This turning point is when the system's total power consumption exceeds the increase in the full rate. Hence, the number of antennas to be selected should not exceed this point to maintain EE; however, finding the optimal point also has its challenge due to processing complexity.



## Distance Aware Transmit Antenna Selection for Massive MIMO Systems

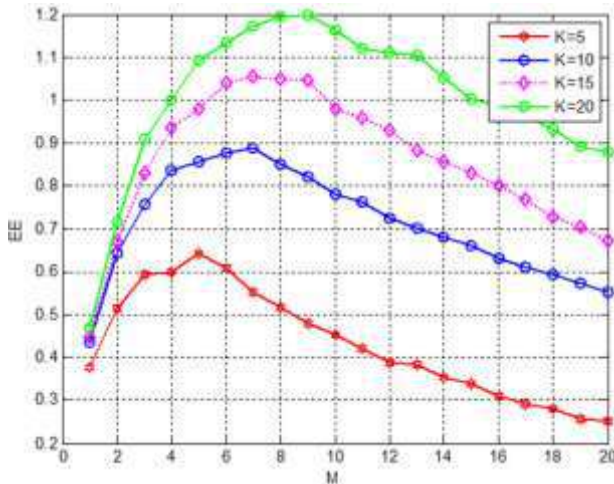


Figure 2: EE at different users and BS antenna settings.

The correlation between energy efficiency,  $k$ , and  $M$  in a massive MIMO system with statistical and instantaneous SNR values is depicted in figure 3. The outcome is evaluated for cell-edge users in LoS settings utilizing algorithm one processes. According to the result, while energy efficiency initially rises as  $M$  increases, it begins to drop at some point as  $M$  keeps growing. For the same  $k$ , statistical and instantaneous or fixed SNR are compared in this figure. Accordingly, fixed SNR outperforms for small  $M$  and comes up short for large  $M$ . It has also been proven that EE grows with user terminals. The EE values for  $k=20$  are obtained from the average value of both statistical and fixed SNR values.

On the other hand, EE presents multiple optimal points due to unpredictable channel circumstances. Furthermore, depending on the number of users and SNR modalities, the ideal EE point for each arrangement differs.

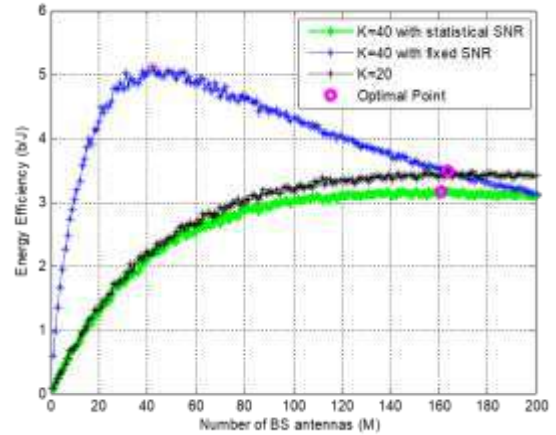


Figure 3: EE for statistical and fixed SNR at sub 6Ghz.

In figure 4, the effect of channel variation on total power and the optimal number of antennas to be selected is shown. When statistical channel variation is considered, the SNR varies. Therefore both total power and  $M^*$  grow large to combat small scale fading by adaptively allocating the desired amount of power. With fixed SNR, fewer antennas can achieve an optimal level than statistical SNR. From the figure, evaluation with statistical SNR accounts for total power consumption than instantaneous SNR assumption, which is 20mW and nearly 19mW for statistical and fixed SNR, respectively.

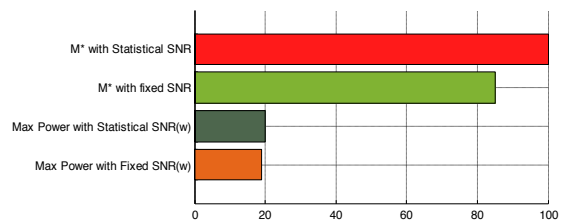


Figure 4: Optimal number of antennas and maximum power for statistical and fixed SNR.

Figures 5 and 6 present the results according to the proposed algorithm by combining the three scenarios, and we have compared the performance of each at CI and FSPL using mmWave and sub 6GHz frequency ranges. The first scenario is finding  $M^*$  from the full array at the indoor cell edge, finding according to (3), and finally evaluating capacity values by combinational permutation as  $\binom{M}{M^o}$ . At the initial access, we assume a deterministic channel, equal power allocation among all BS antenna elements and the point at which the EE graph starts diminishing is evaluated using the reference signal. Then the number of antennas at that point is used as a baseline for our further considerations. Before the energy efficiency evaluation process, we make the analysis of free space and CI path loss models according to their formulations stated in (1) and (2).

Accordingly, the FS model provides higher data rates due to obstruction; however, CI is more realistic than FS in practical scenarios. Based on this intuition, we have applied an antenna selection algorithm for both, and the results show that a much smaller number of antennas are selected in free space than CI. Besides, when CI path loss is applied to mmWave and sub 6GHz frequency ranges and reached for fixed total system power, CI with sub 6GHz is more energy-efficient than mmWave. Despite high-frequency signals carrying larger data than low-frequency signals, as frequency increases, the blockage due to different impairments also exhibits low wavelength, which negatively affects the received signal.

Low received signal accounts for low data rate at the receiver, and thus EE is degraded compared to CI. Finally, we have found that the FS path loss with the DPC precoder changes the graph from logarithmic to almost linear and starts an abrupt shift to decline after the maximum point. However, it is limited to the total value in this case.

Figure 5 depicts minimum SNR-based antenna selection using linear and nonlinear precoders and compares with EE at full array implementation with no precoders. After finding an optimal number of antennas, as figure 5, it applies (3) to recalculate a new optimal point that depends on the users' current position or distance and adaptive reduction of  $M$  instead of transmitting power. In this case, the optimal, which was found in full array implementation, is used as  $M$  to re-search the new optimal value (3). Despite the reduction in the total rate when the number of antennas is reduced, the reduction in total power consumption compensates for maintaining EE. Finally, applying precoders in general and nonlinear DPC, in particular, boosts the total rate of the system and EE as well. We have evaluated EE as a function of BS antennas at different power levels for full array and selection implementations. The performance of the system has also been assessed with and without the nonlinear precoding and shown that antenna selection with minimum SNR significantly improves the energy efficiency with less transmit power and DPC precoder.

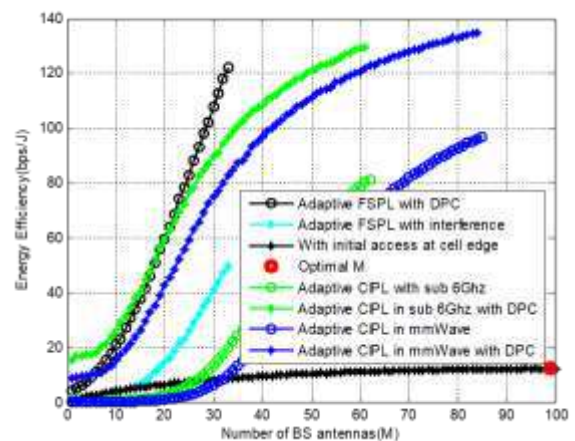


Figure 5: Energy efficiency evaluation as a function of number of BS antennas with at mmWave frequency,  $f=38$  GHz  $M=64$ .

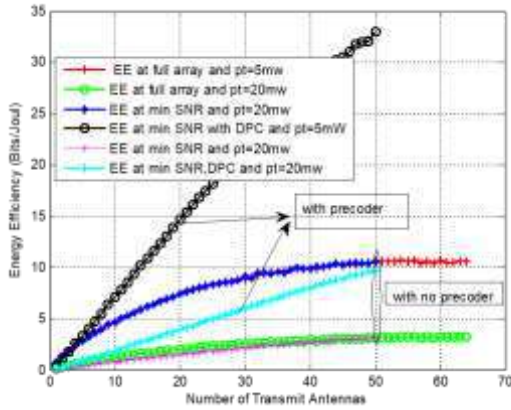


Figure 6: Energy efficiency evaluation as a function of number of BS antennas with mmWave frequency,  $f=38$  GHz  $M=64$ .

The complex nature of the proposed selection algorithm is shown in figure 7, and it is compared with the works that employ comparable strategies. The number of iterations of the main and nested loops that must occur when selecting the branch with the best channel gain among the complete array is referred to as complexity in this scenario. On the other hand, random selection is minor complex, despite having a lesser capacity than complex selection, as shown in the graph. This is because the selection is made regardless of channel gain, which is critical in increasing capacity and complexity.

For random selection, the number of iterations to select  $M$  antennas is only one as it has no combination with the channel branches. Our proposed algorithm is also compared with [16], [17], and [18], which are among the simplest and follow similar approaches to the best of our knowledge. The complexity order of each is our proposed technique and random selection according to (17), (18), and (19). We have also found that the proposed algorithm is more energy-efficient than random at the cost of some complexity which is less than that of [16] and [19]. Moreover, the energy efficiency of the proposed technique has

been shown to surpass random selection, full array utilization, and some other literature, as shown in the figure. However, the effect and trade-off rate, including EE of the literature above, is left as our future work.

Therefore, the selection technique meets our primary goal of proposing an energy-efficient system at manageable complexity.

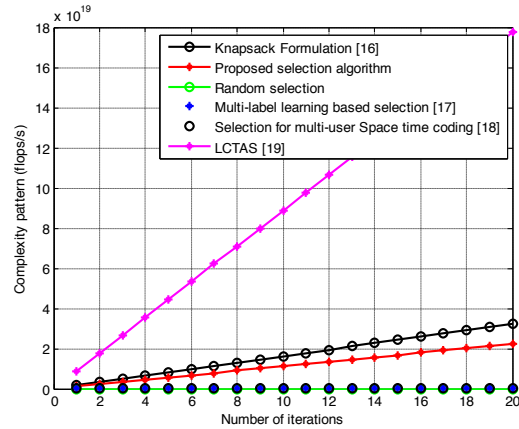


Figure 7: Computational complexity of selection algorithms with adaptively selected number of elements and  $M=64$ .

## CONCLUSIONS

This work has focused on the problem of system energy efficiency due to the massive number of antenna elements to be installed on a single BS in the upcoming wireless communication era. Adaptive antenna selection technique has been proposed as a novel strategy in resolving a substantial amount of power consumption and complexity as a result of power-hungry RF elements which grow with antenna elements. The selection has been made for cell-edge users with a full array at fixed power allocation and minimum SNR-based selection for cell center users. Both cases are used to achieve the optimal number of antennas at which EE becomes maximum. The key idea of the proposed algorithm is to minimize the number of RF chains, and performance evaluation has been done in

several scenarios by applying precoders at different frequency ranges. The numerical results show that the proposed antenna selection algorithm performs better than full utilization of the array while finding some computational complexity when applying nonlinear precoders to compensate the total rate whilst selection gets negative effects. Moreover, we have evaluated the complex pattern of previous and current works with similar techniques. Accordingly, it has been shown that the proposed approach is least complicated and energy-efficient compared to the Knapsack formulation and LCTAS.

### REFERENCES

- [1] Larsson E., Tufvesson G., F., Edfors O., and Marzetta T. L., "Massive MIMO for next generation wireless systems," *CoRR*, vol. abs/1304.6690, 2013.
- [2] Heath R.W., Sandhu S., and Paulraj A., "Antenna selection for spatial multiplexing systems with linear receivers," *IEEE Commun. Lett.*, vol. 5, no. 4, pp. 142-144, Apr. 2001.
- [3] Correia L., Zeller D., Blume O., Ferling D., Jading Y., Godor L., Auer G., and Van der Perre L., "Challenges and enabling technologies for energy aware mobile radio networks," *IEEE Communications Magazine*, vol. 48, no. 11, pp. 6672, November 2010.
- [4] Heath R.W., Sandhu S., and Paulraj A., "Antenna selection for spatial multiplexing systems with linear receivers," *IEEE Commun. Lett.*, vol. 5, no. 4, pp. 142-144, Apr. 2001.
- [5] Gharavi-Alkhansari M., and Gershman A.B., "Fast Antenna Subset Selection in MIMO Systems," *IEEE Trans. Signal Process.*, vol. 52, no. 2, pp. 339-347, Feb. 2004.
- [6] Dua A., Medepalli K., and Paulraj A.J., "Receive Antenna Selection in MIMO Systems Using Convex Optimization," *IEEE Trans. Wireless Commun.*, vol. 5, no. 9, pp. 2353-2357, Sept. 2006.
- [7] Wang B.H., Hui H.T., and Leong M.S., "Global and Fast Receiver Antenna Selection for MIMO Systems," *IEEE Trans. Commun.*, vol. 58, no. 9, pp. 2505-2510, Sept. 2006.
- [8] Xu Z., Sfar S., and Blum R. S., "Analysis of MIMO systems with receive antenna selection in spatially correlated Rayleigh fading channels," *IEEE Trans. Veh. Technol.*, vol. 58, no. 1, pp. 251262, Jan. 2009.
- [9] Masouros C. and Alsusa E., "Dynamic linear precoding for the exploitation of known interference in MIMO broadcast systems," *IEEE Transactions on Wireless Communications*, vol. 8, no. 3, pp. 1396-1404, March 2009.
- [10] Gesbert R., "Soft linear precoding for the downlink of DS/CDMA communication systems," *IEEE Transactions on Vehicular Technology*, vol. 59, no. 1, pp. 203-215, January 2010.
- [11] Xiang G.; Edfors, Ove; Liu, Jianan; Tufvesson, Fredrik, "Antenna selection in measured massive MIMO channels using convex optimization," *IEEE GLOBECOM Workshop*, 2013, Atlanta, Georgia, United States.
- [12] Gao X., Edfors O., Rusek F., and Tufvesson F., "Massive MIMO performance evaluation based on measured propagation data," *IEEE Transactions on Wireless Communications*, vol. 14, no. 7, pp. 3899-3911, July 2015.

## Distance Aware Transmit Antenna Selection for Massive MIMO Systems

- [13] Rappaport T. S., *Wireless Communications: Principles and Practice*, 2nd ed," *Upper Saddle River*, NJ: Prentice Hall, 2002.
- [14] Rappaport T. S. et al., "Wideband millimeter-wave propagation measurements and channel models for future wireless communication system design (Invited Paper), *IEEE Transactions on Communications*," vol. 63, no. 9, pp. 3029-3056, Sep. 2015.
- [15] Guthy C., Utschick W., and Honig M., "Large system analysis of sum capacity in the gaussian MIMO broadcast channel," *IEEE Journal on Selected Areas in Communications*, vol. 31, no. 2, pp. 149-159, Feb. 2013.
- [16] Husbands R., Ahmed Q., and Wang J., "Transmit Antenna Selection for Massive MIMO: A Knapsack Problem Formulation," *IEEE ICC 2017 Wireless Communications Symposium*, Jan, 2017.
- [17] Yu W., Wang T. and Wang S., "Multi-Label Learning Based Antenna Selection in Massive MIMO Systems," DOI 10.1109/TVT.2021.3087132, *IEEE Transactions on Vehicular Technology*, June 09, 2021.
- [18] Kim S., "Efficient Transmit Antenna Subset Selection for Multiuser Space-Time Line Code Systems," *Sensors* 2021, 21, 2690. <https://doi.org/10.3390/s21082690>.
- [19] Pillay N., Xu H. , "Low-complexity transmit antenna selection schemes for spatial modulation," *IET Commun.*, 2015, Vol. 9, Iss. 2, pp. 239–248 doi: 10.1049/iet-com.2014.0650.